



Tour des méthodes de mesure d'élévation par imagerie SAR : de la radargrammétrie à la tomographie

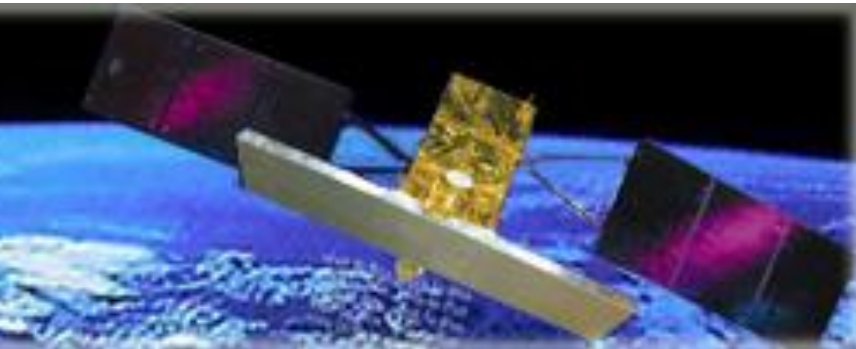
J.-M. Nicolas, F. Tupin
Télécom ParisTech – LTCI



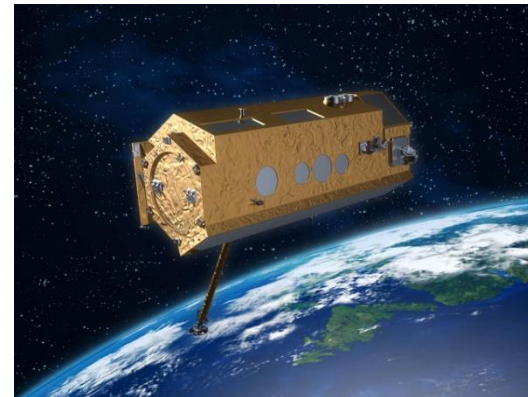
Journée thématique du PNTS –
Observation et modélisation de structures 3D des enveloppes superficielles
16 mars 2017

Context

- Golden age of SAR sensors: improved spatial, polarimetric and temporal resolutions



CSK



TerraSAR-X

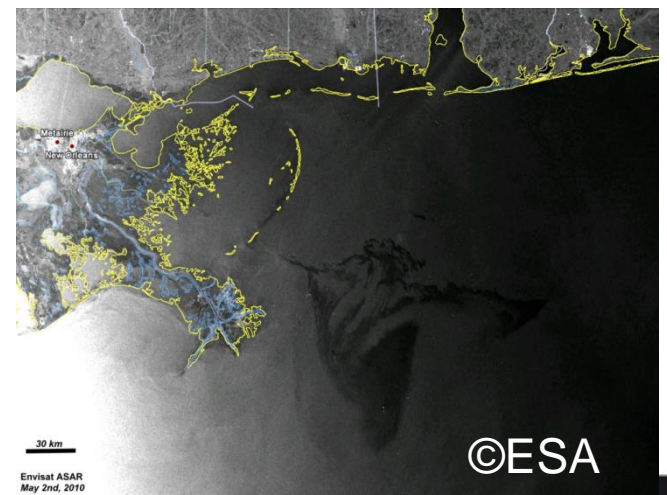
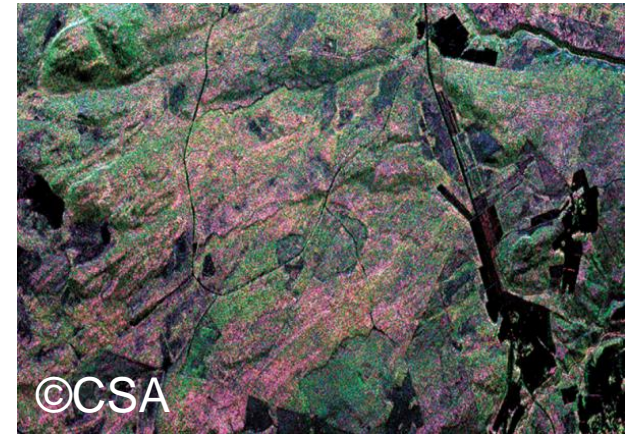
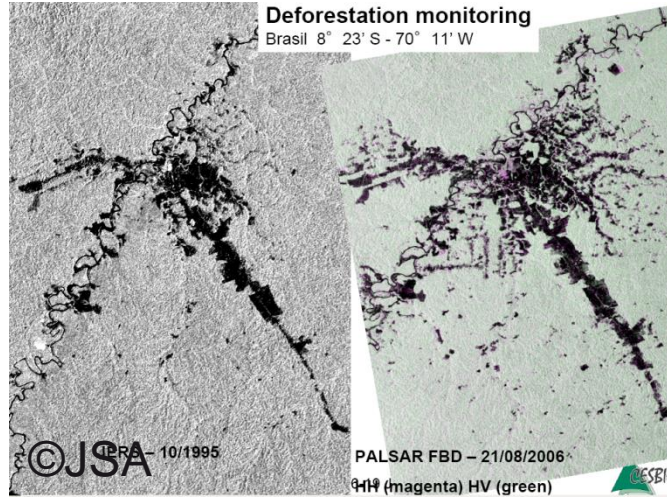
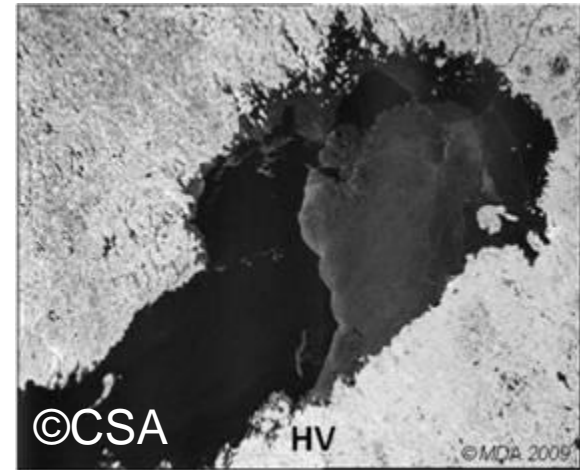


Sentinel I

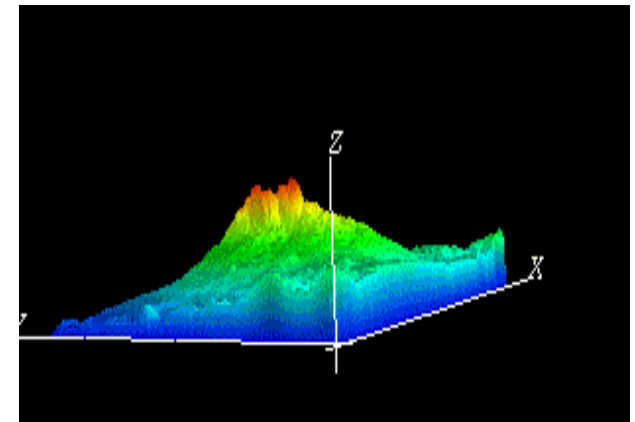
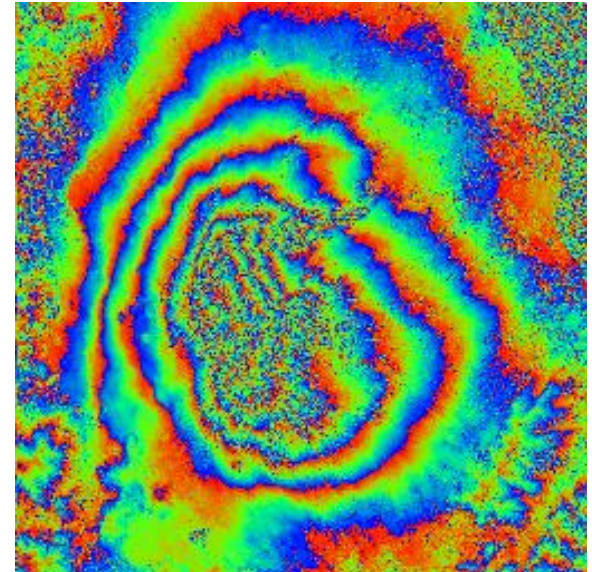
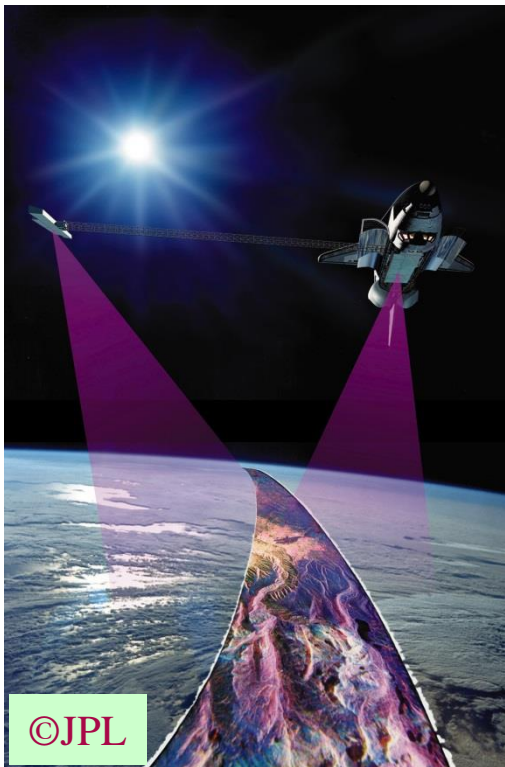


RadarSAT-2

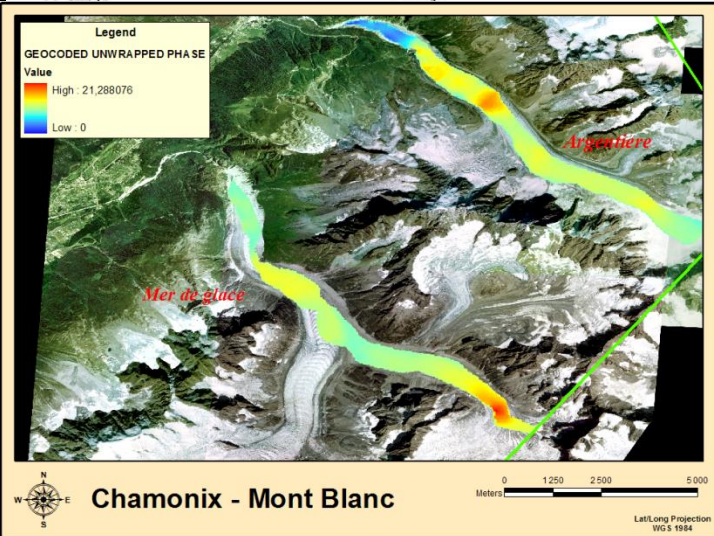
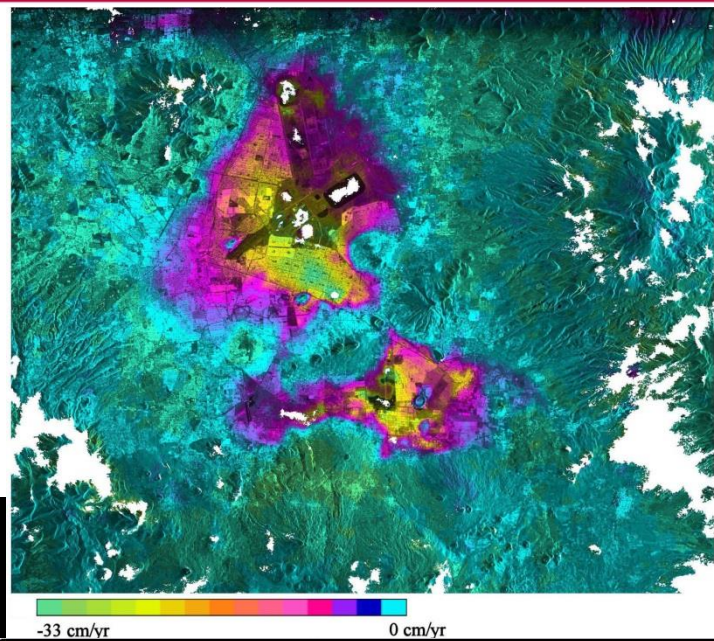
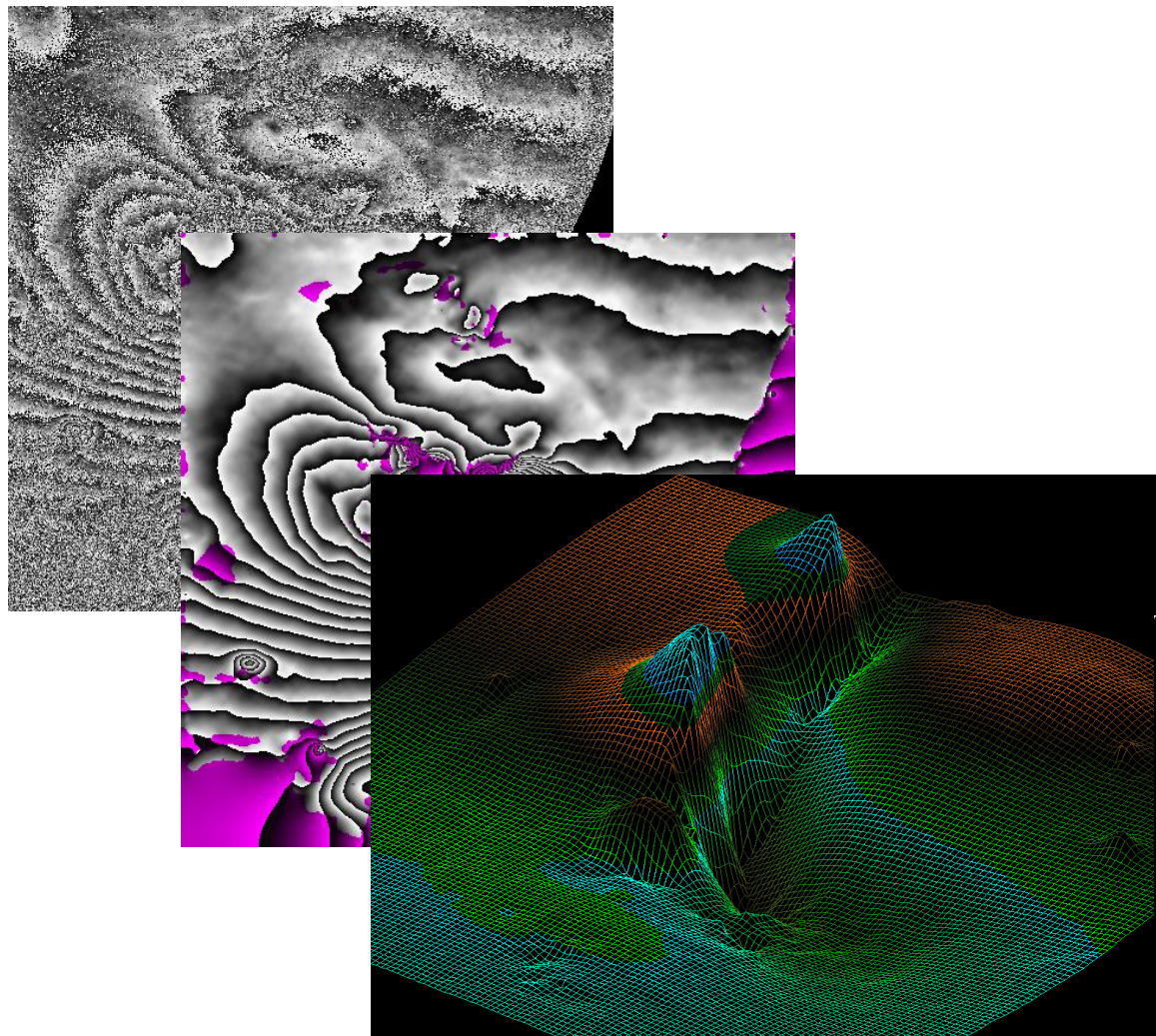
Context



Context



Context



Overview

■ How recovering elevation information ?

- Radargrammetry
- Interferometry
- Tomography

■ Focus on urban areas

- Geometric limits
- Use of external information

■ How helping with image processing ?

- Data and prior models
- Fusion of information

■ Conclusion



Data acquisition

■ SAR signal: complex signal

- Amplitude: backscattering coefficient of the scene
- Phase: linked to the geometry



■ Elevation: 1, 2 or more images

- *Radarclinometry (amplitude)*
- Stereoscopy (amplitude)
- Interferometry (phase)
- Tomography (n-D phase)

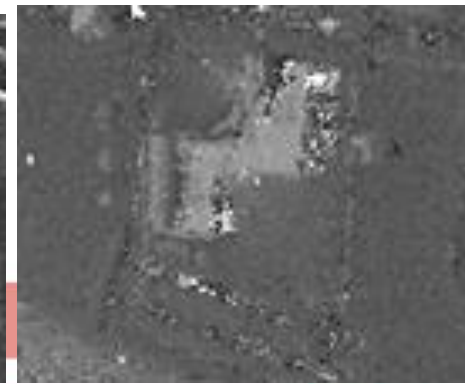
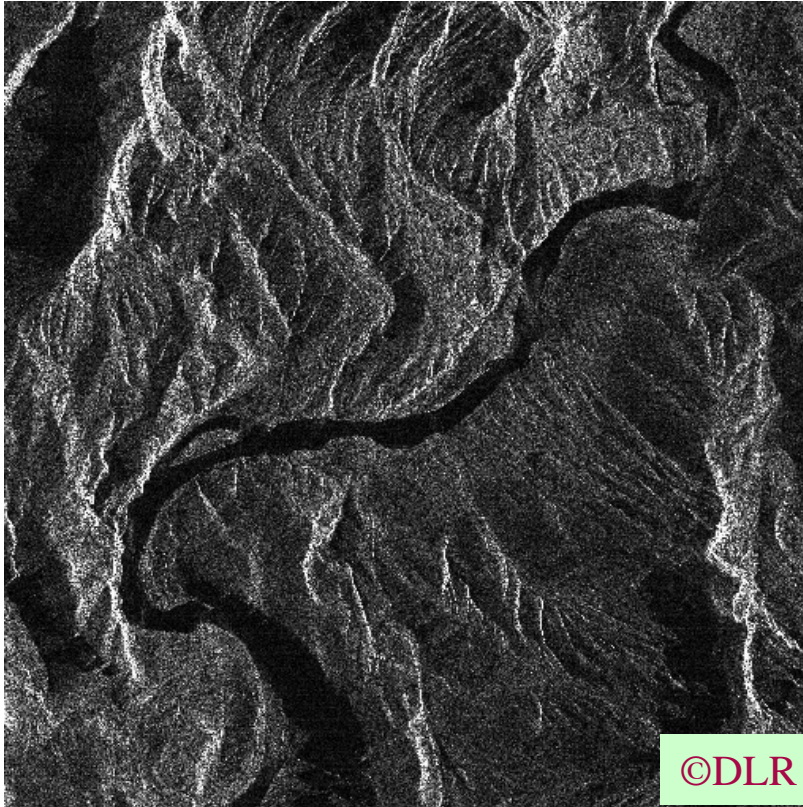
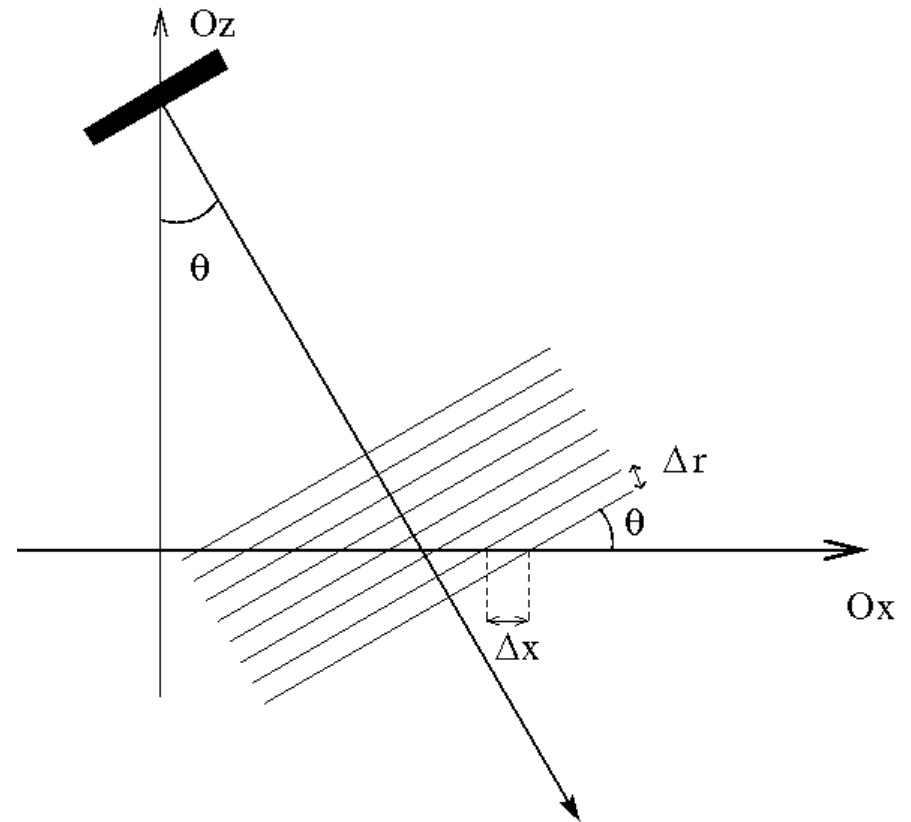
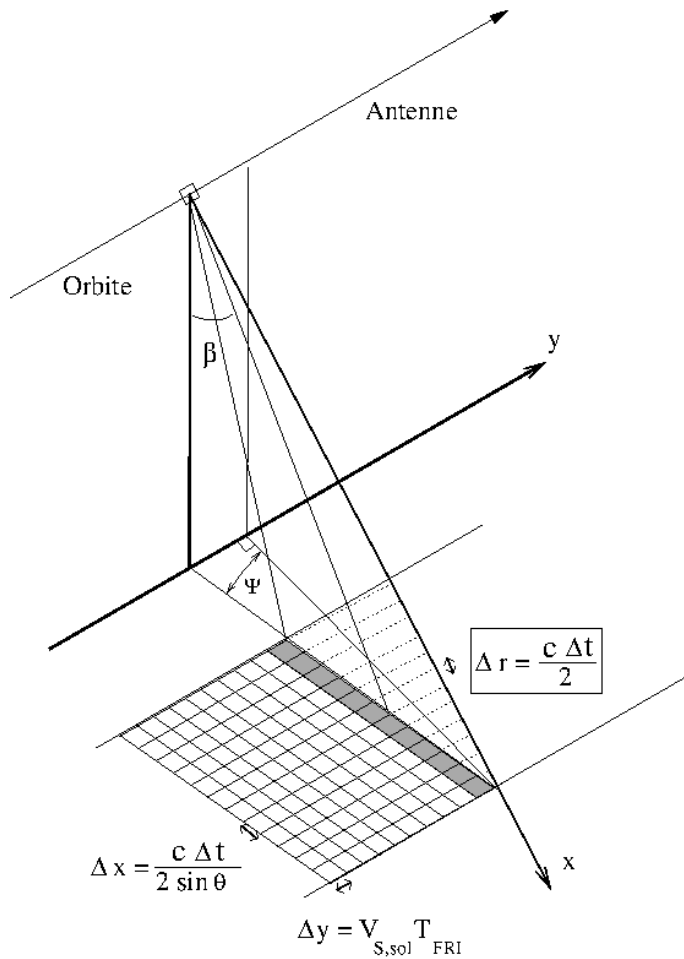


Image Terrasar-X



- Visée latérale : effets liés au relief
- Imagerie cohérente : chatoiement
- Réponse (RCS) pour des longueurs d'onde centimétriques

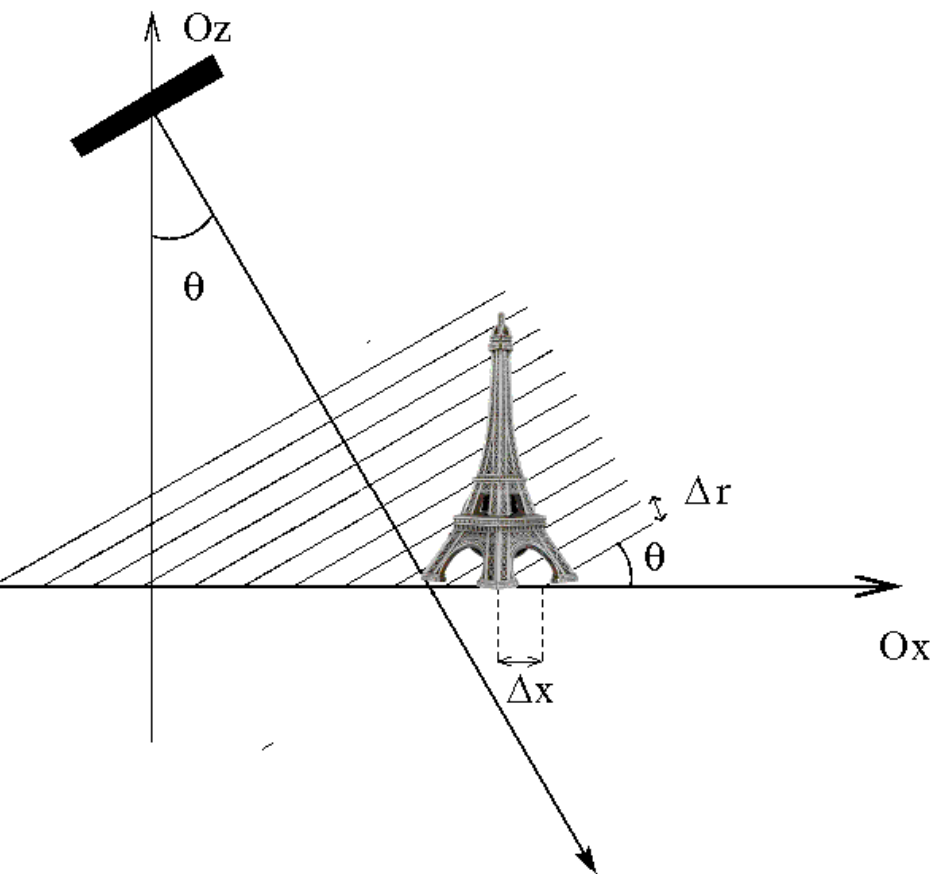
Construction d'une image Radar



Tout est géométrie !!

Acquisition SAR

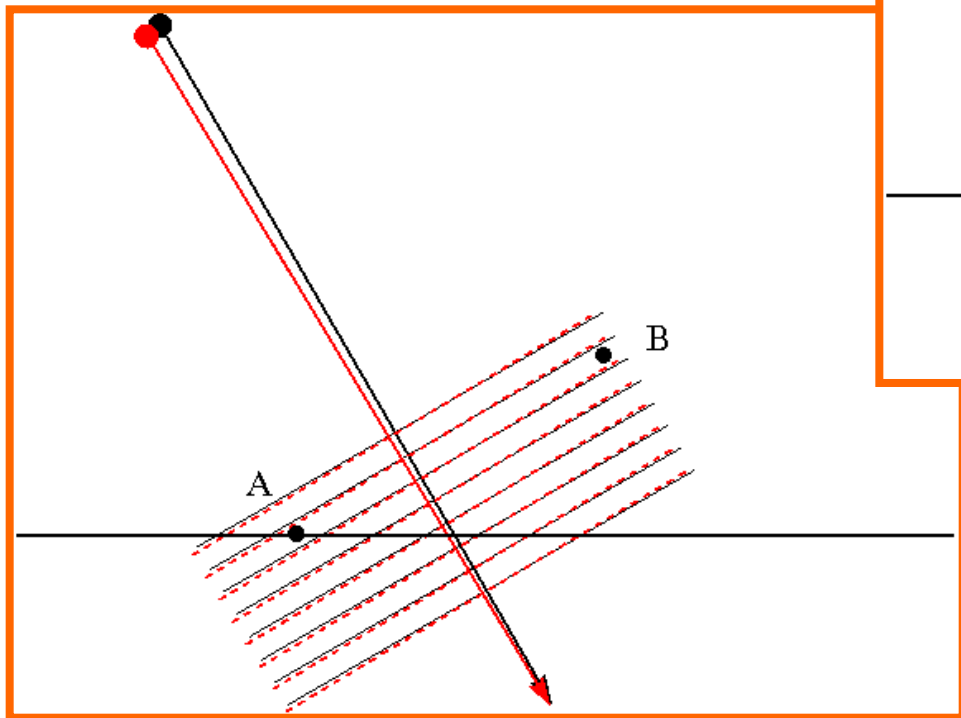
■ Terrasar-X, $\theta \sim 30^\circ$



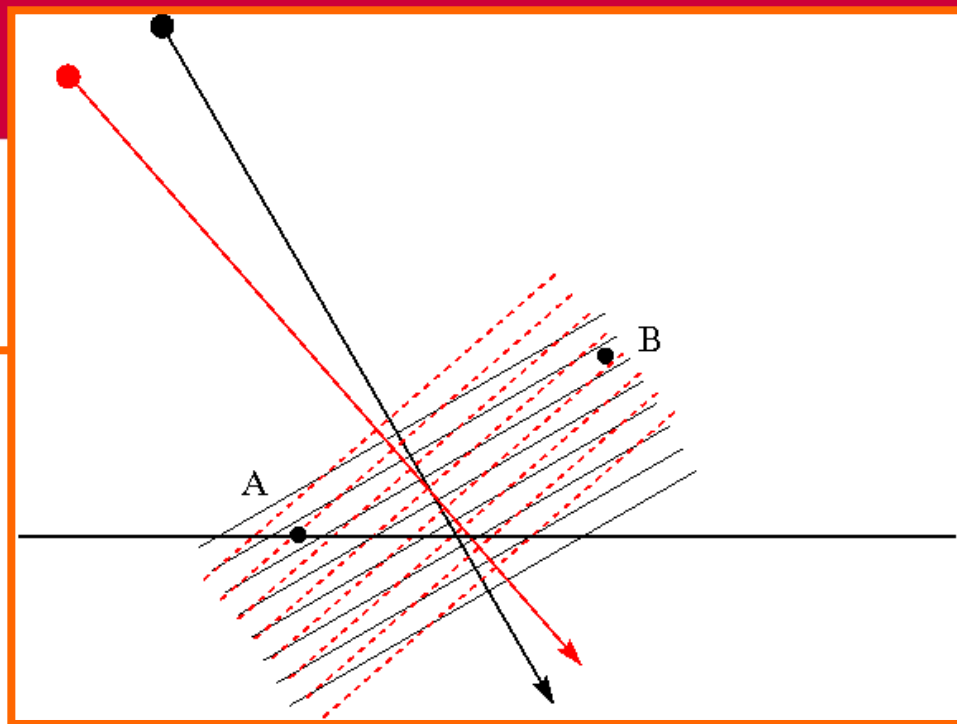
©DLR

TELECOM
ParisTech





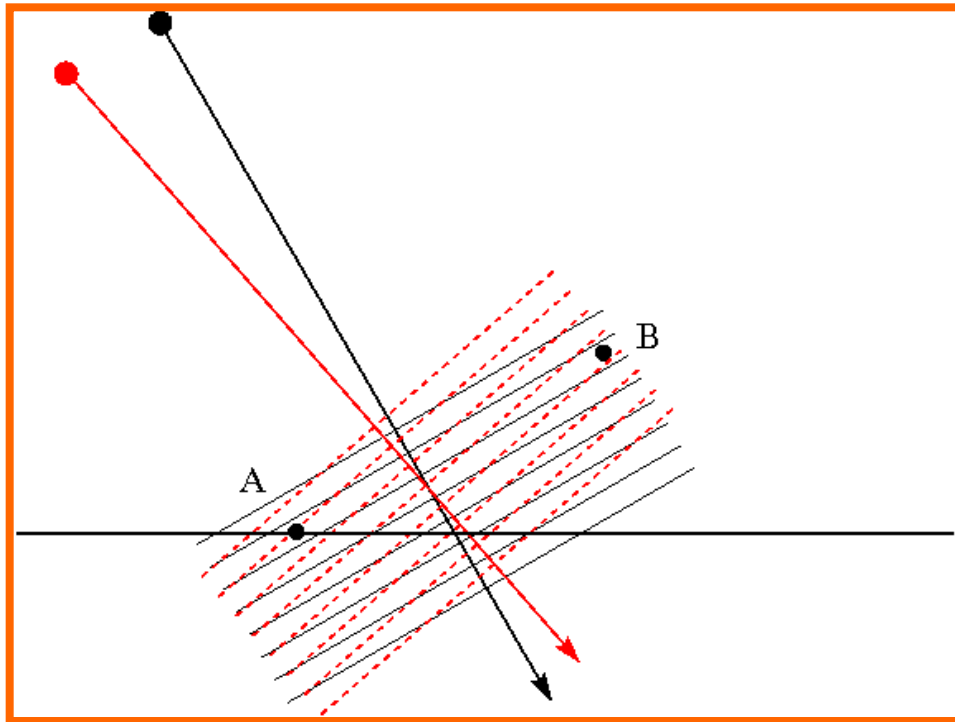
Petite base :
Interférométrie



Grande base :
Radargrammétrie

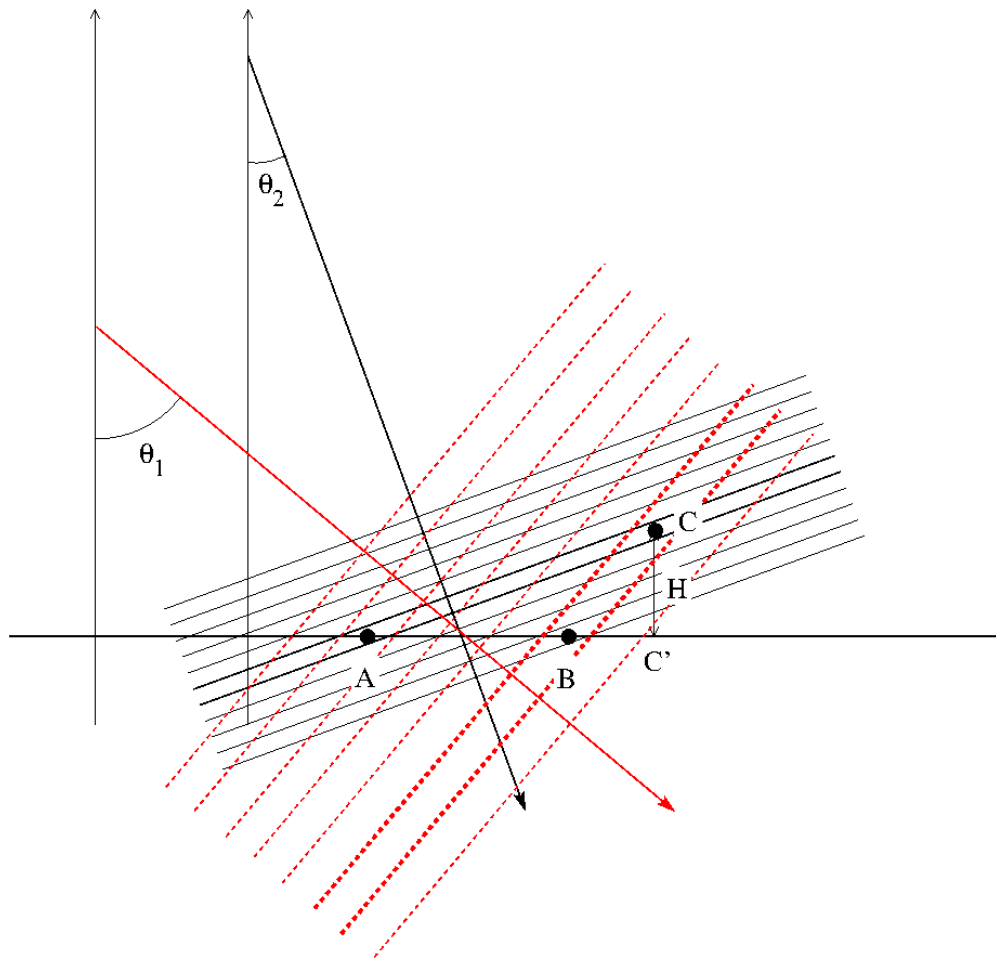
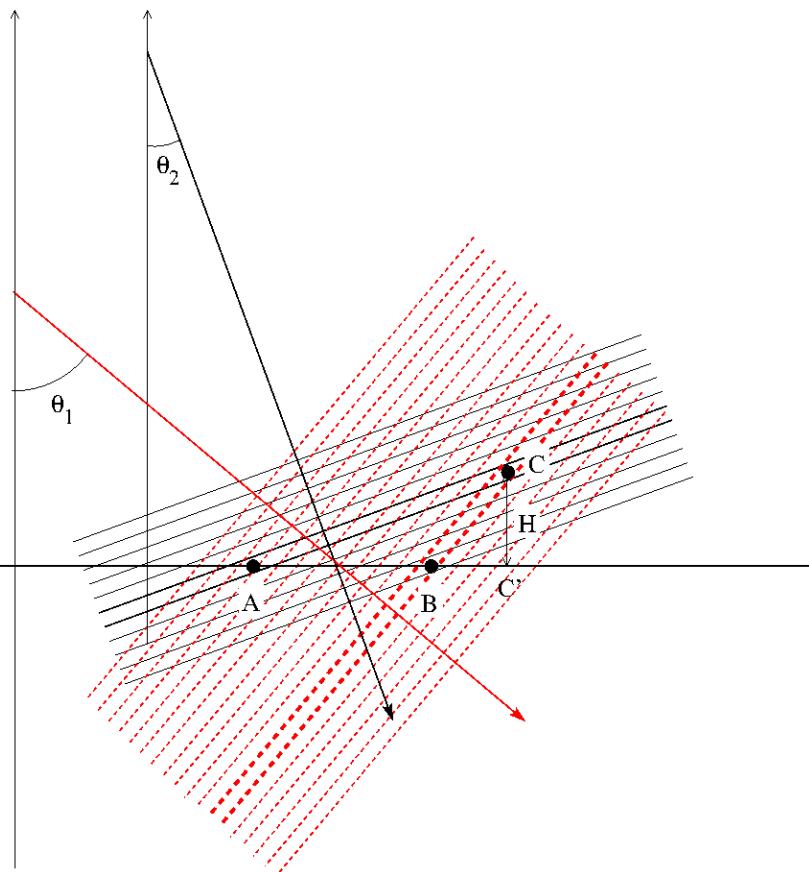
Grande base

Deux antennes avec des incidences différentes



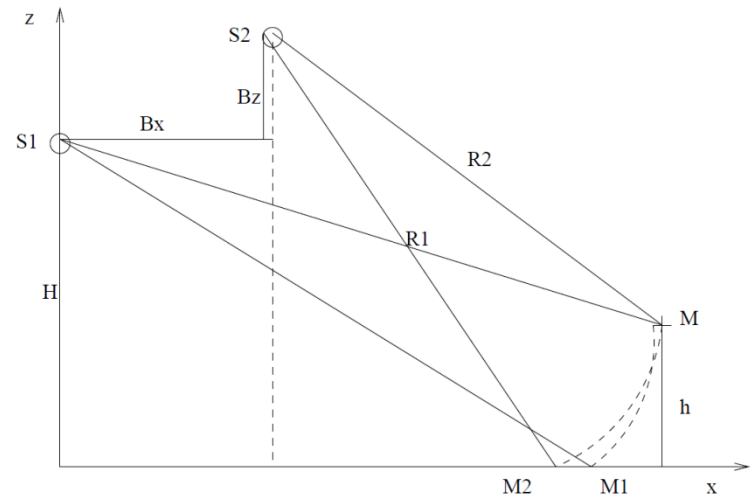
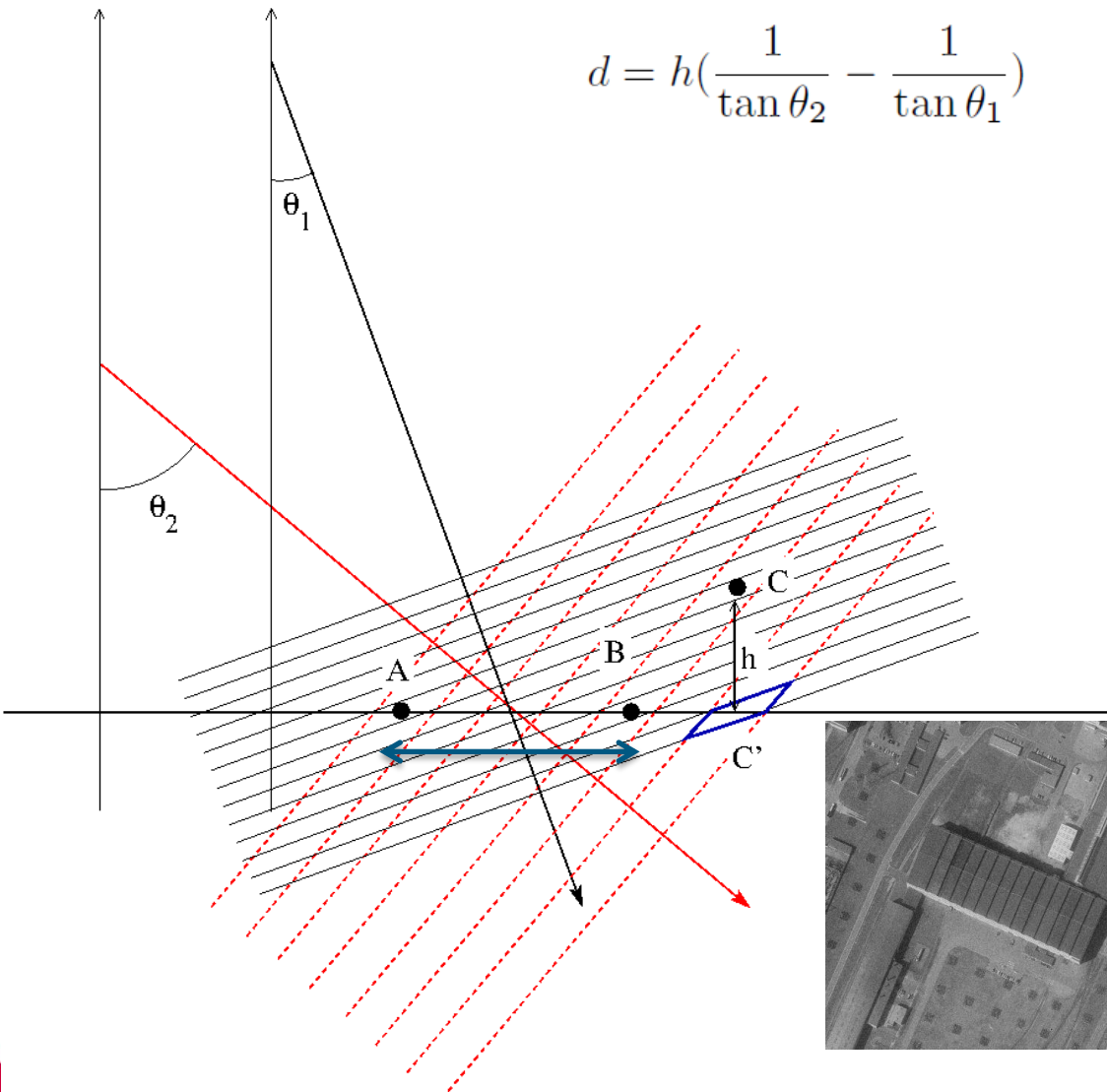
- Deux objets A et B
- Dans la même case distance pour l'antenne noire
- Dans deux cases distance de l'antenne rouge !!
- →stéréoscopie

Recalage : même pixel sol



Radargrammétrie

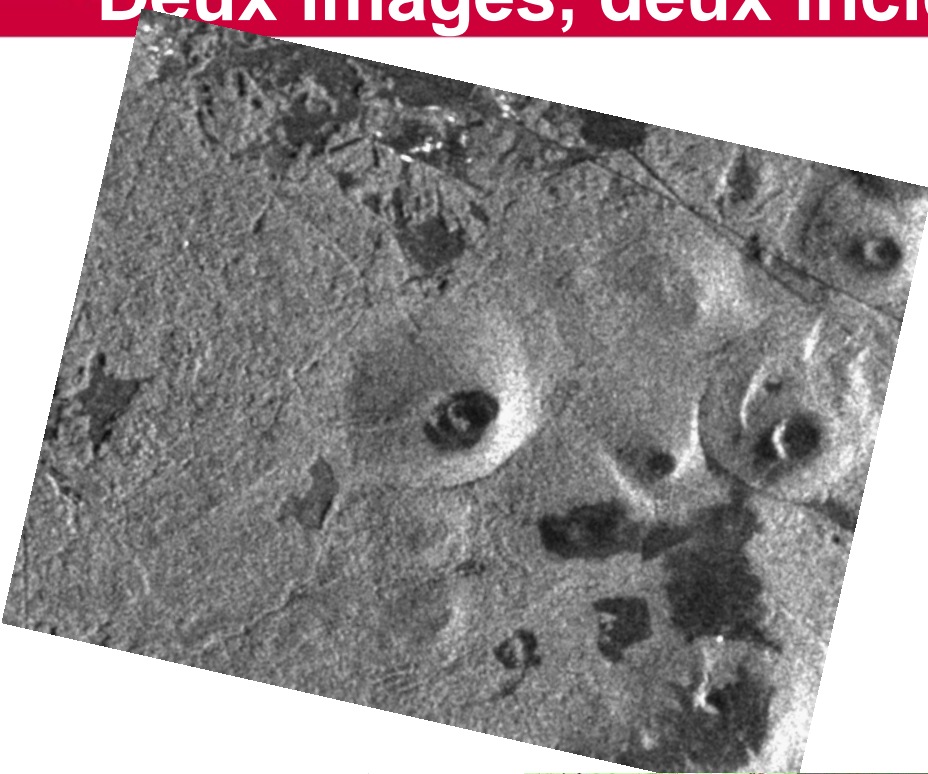
$$d = h \left(\frac{1}{\tan \theta_2} - \frac{1}{\tan \theta_1} \right)$$



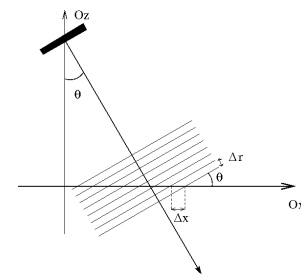
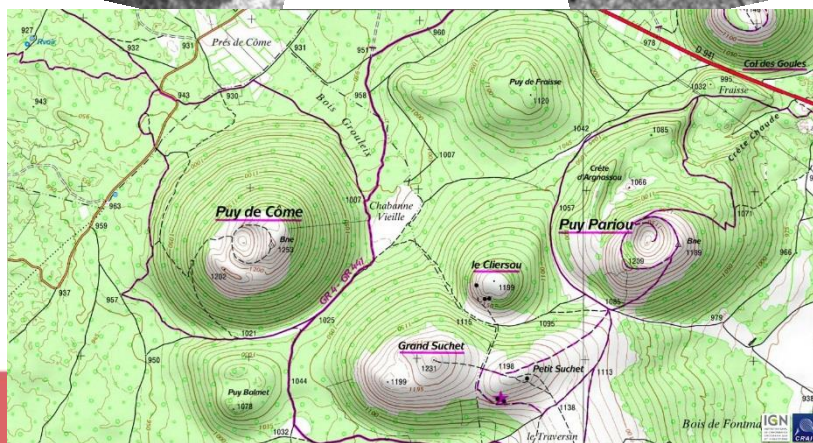
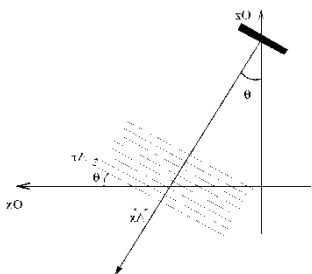
©ONERA/CNES



Deux images, deux incidences



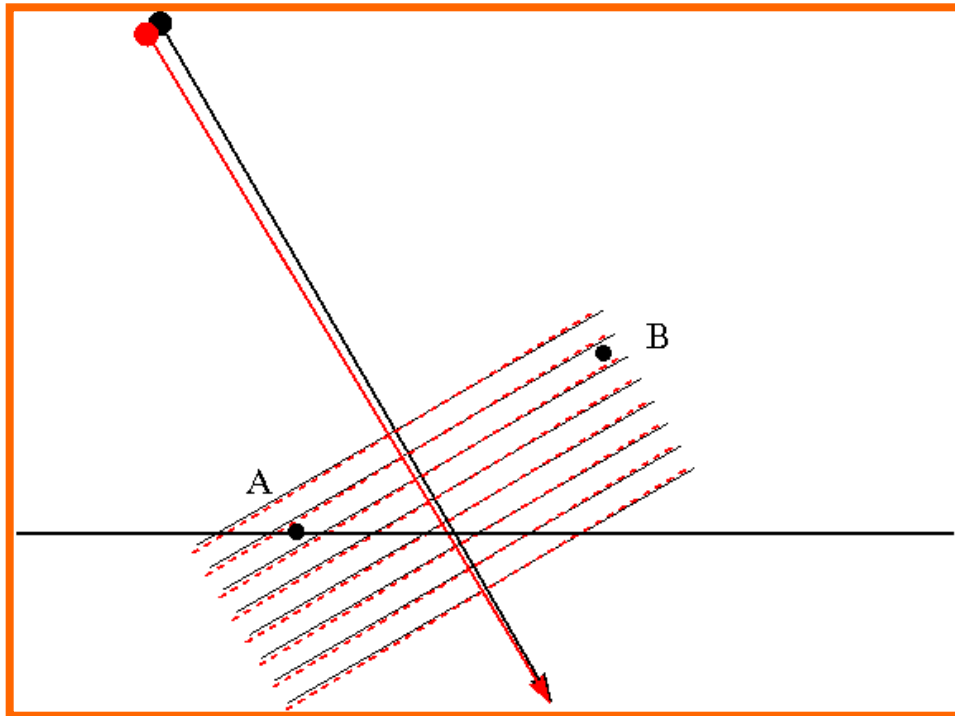
©ESA



Images Sentinel

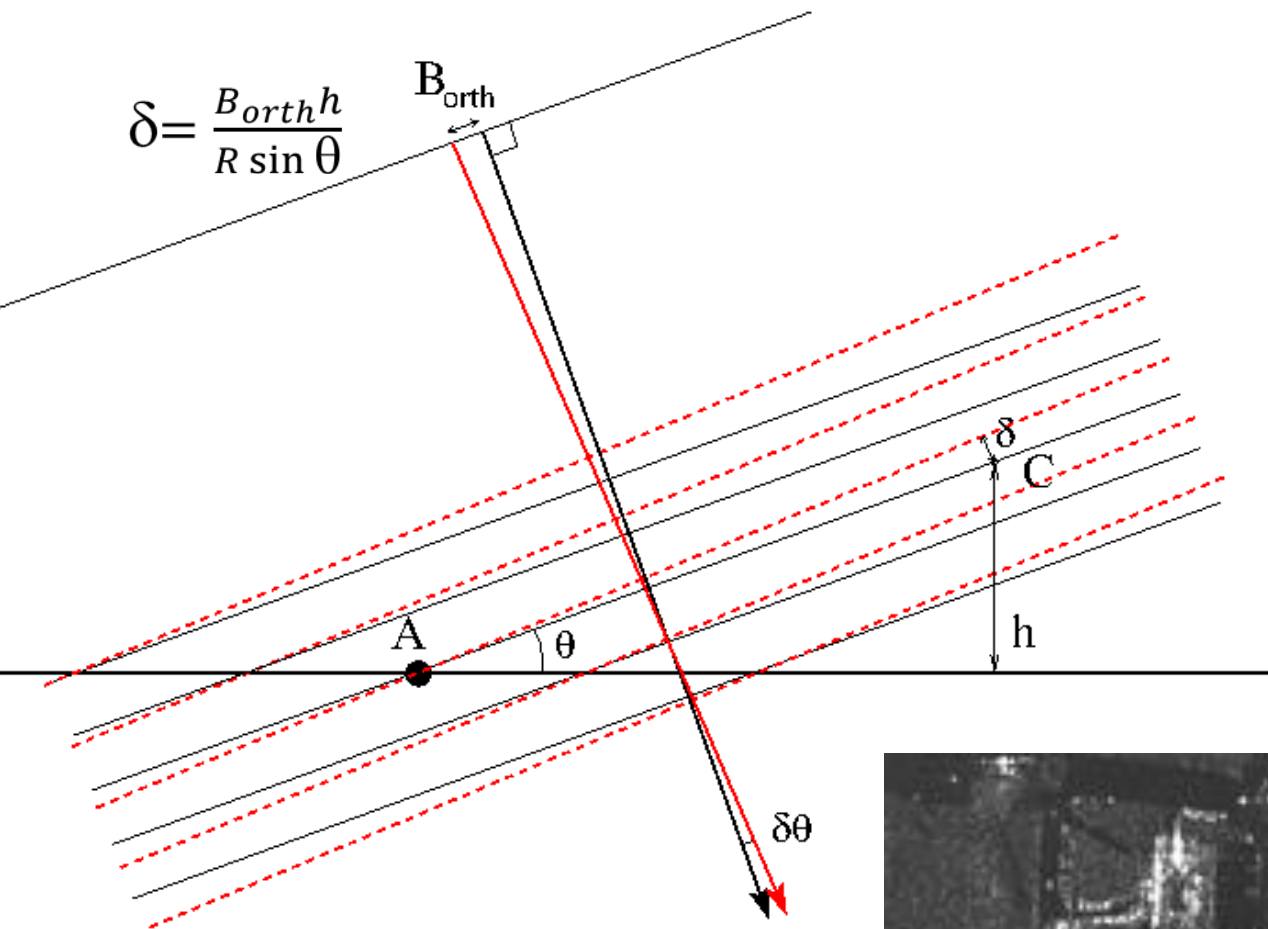


Petite base : deux antennes avec presque la même incidence



- Deux objets A et B
- Dans la même case distance pour l'antenne noire
- Dans la même case distance de l'antenne rouge
- → interférométrie

Interférométrie

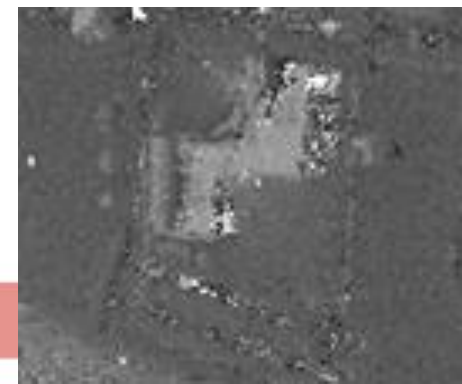


$$\phi = \frac{4\pi R}{\lambda} + \phi_{pr}$$

$$\phi_2 - \phi_1 = \frac{4\pi(R_2 - R_1)}{\lambda} = \psi_{1,2}$$

$$\psi_{1,2} = \frac{4\pi B_{\perp 1,2}}{R \sin(\theta) \lambda} h$$

$$\psi_{1,2} = \alpha_{geom 1,2} h$$

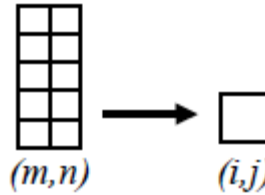


SAR interferometric data

■ Interferometry:

$$z_1(m, n) = A_1(m, n)e^{i\phi_1(m, n)}$$

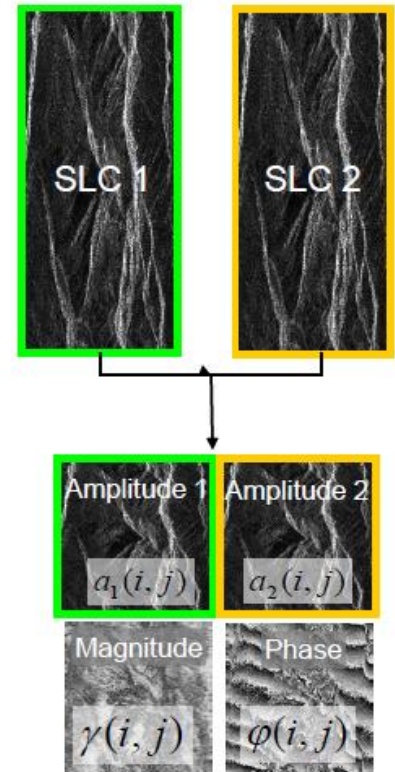
$$z_2(m, n) = A_2(m, n)e^{i\phi_2(m, n)}$$



$$\gamma(i, j)e^{i\phi(i, j)} = \frac{\sum_{(m, n)} z_1(m, n)z_2^*(m, n)}{\sqrt{\sum_{(m, n)} |z_1(m, n)|^2} \sqrt{\sum_{(m, n)} |z_2(m, n)|^2}}$$

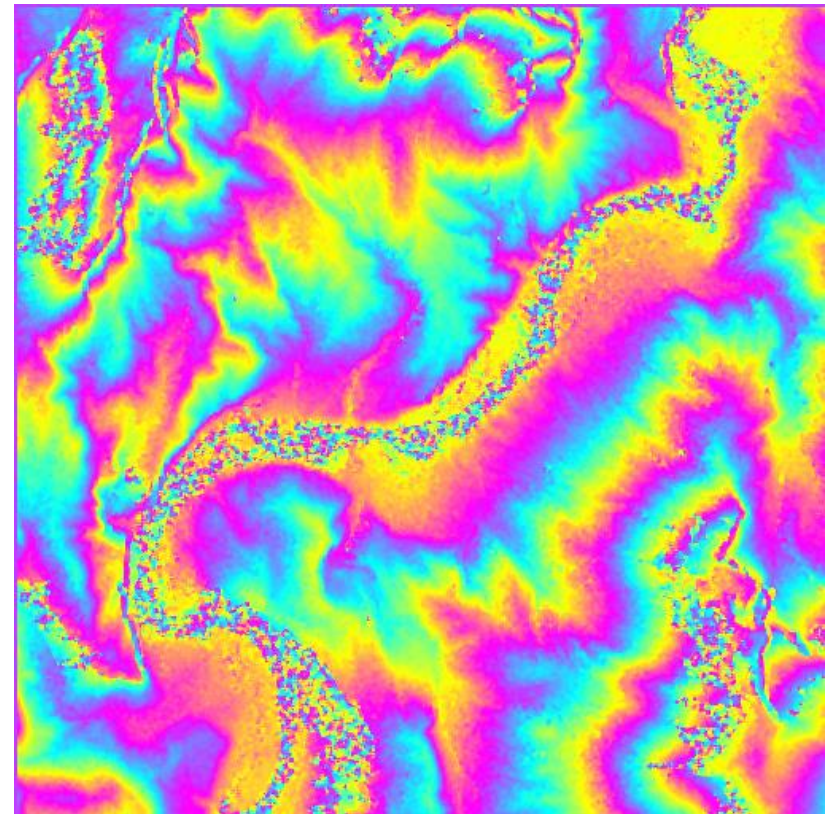
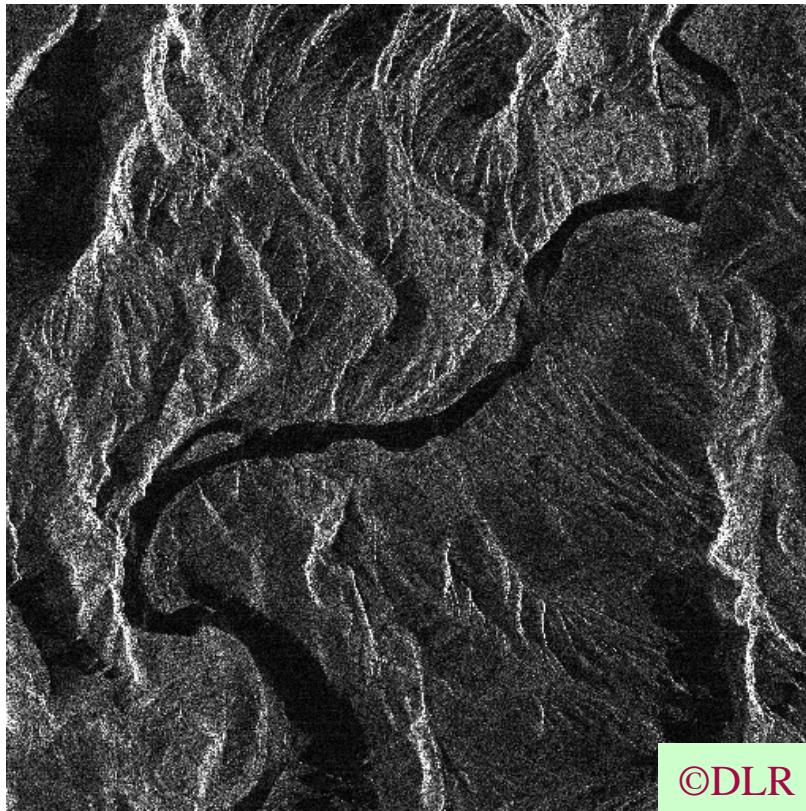
■ Multi-temporal InSAR:

- Topography + displacement (D-InSAR)
- Perturbations:
 - Phase decorrelation noise
 - Systemic errors (atmosphere, orbit,...)



Mesure du relief

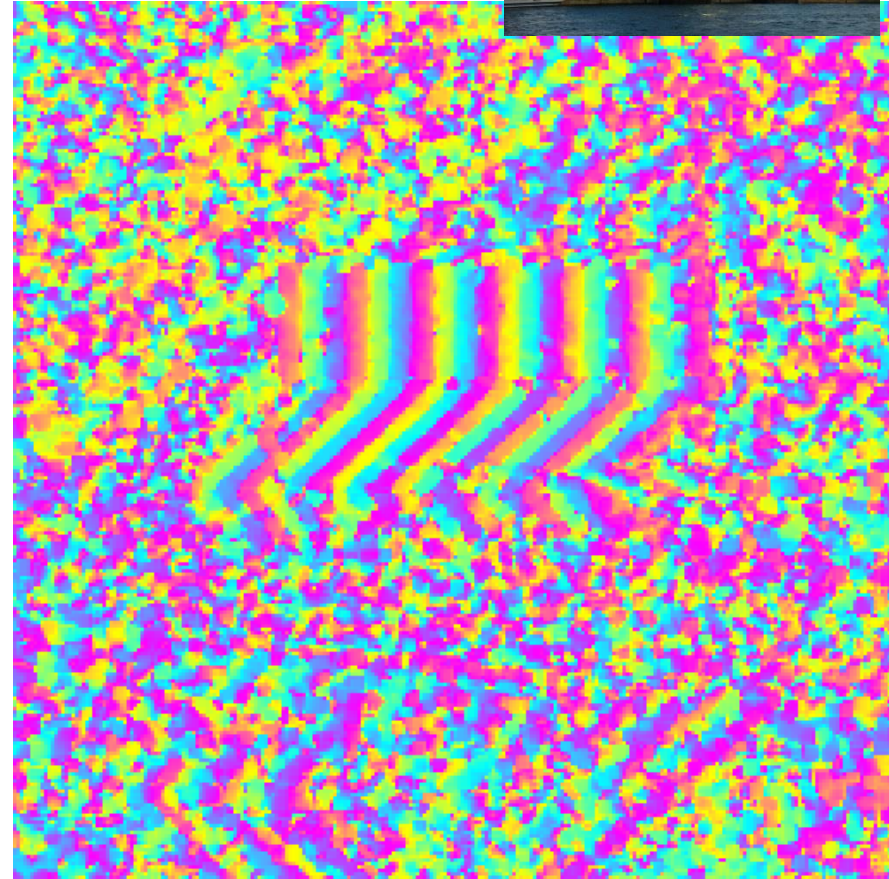
Grand canyon du Colorado



Tour Mirabeau (70m) Mesure de $\delta\varphi$



©DLR



Environ 6 franges : Base orthogonale de 473m. Altitude estimée : 69m

Comparaison - intérêts / limites

■ Radargrammétrie

- Mise en correspondance *éparse*
- Variations de rétrodiffusion en fonction de l'angle
- Précision de reconstruction

$$\epsilon \approx \frac{1}{\sin(\delta\theta)}$$

■ Interférométrie

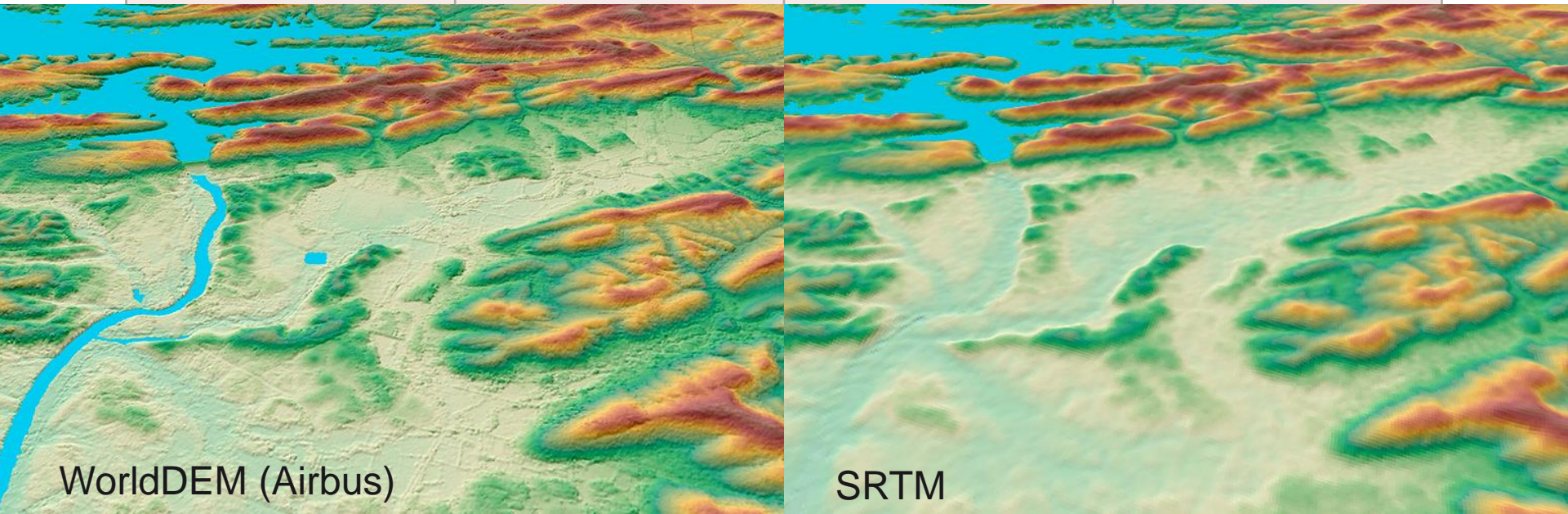
- Mise en correspondance *dense*
- *Décorrélation* spatiale, temporelle, perturbations atmosphériques
- Difficultés de *déroulement* de la phase (altitude d'ambiguïté)

$$h_{amb} = \frac{\lambda R \sin \theta}{2B_{\perp 1,2}}$$

$$\sigma_h = \sigma_\psi \frac{h_{amb}}{2\pi}$$

Reconstruction 3D - MNT

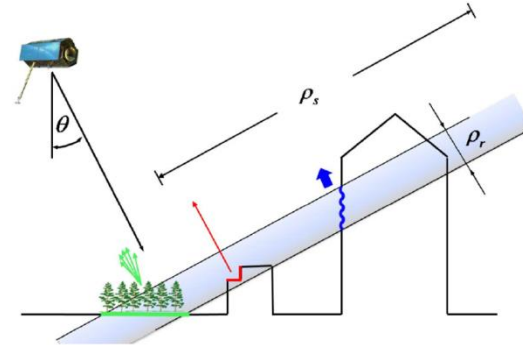
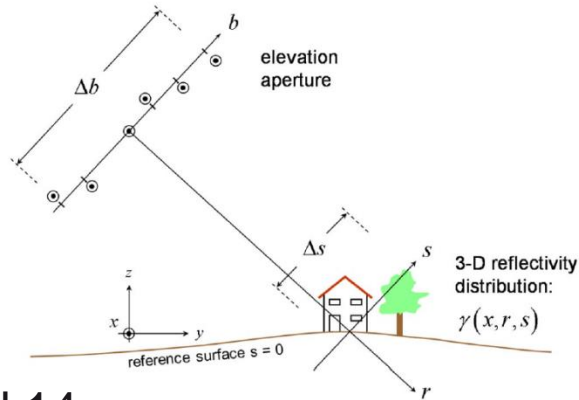
Mission	mode	Précision planimétrique	Précision altimétrique
SRTM (2000)	Bande X Interféro mono-passe	60m (30m)	16m abs. 10m rel.
TanDEM-X WorldDEM	Interféro mono-passe + multi-passe	12m	4m abs. 2m rel.



WorldDEM (Airbus)

SRTM

Tomographie SAR



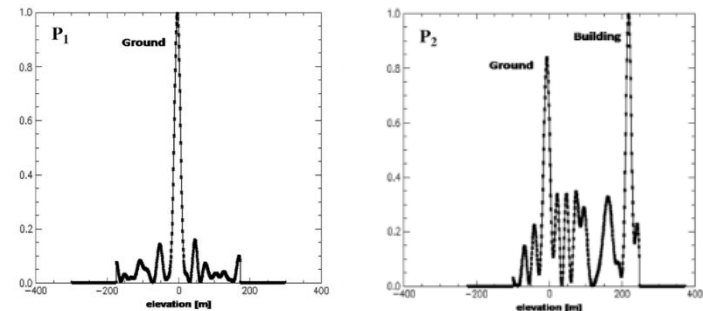
Zhu et al.14

$$g_n = \int_{\Delta s} \gamma(s) \exp(-j2\pi\xi_n s) ds, \quad n = 1, \dots, N$$

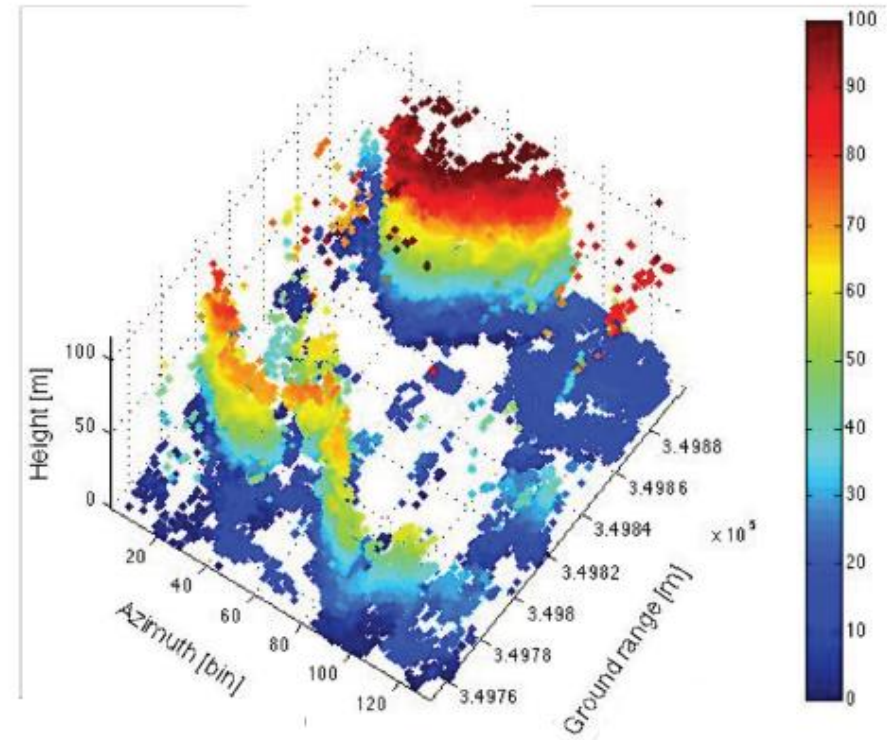
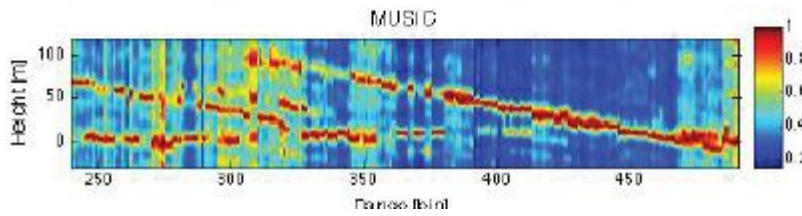
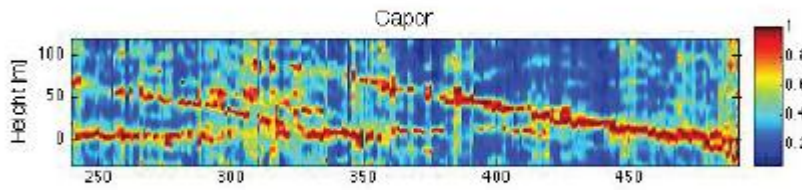
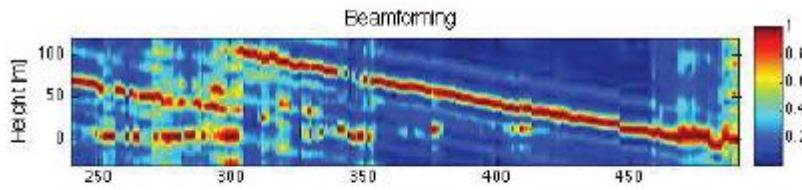
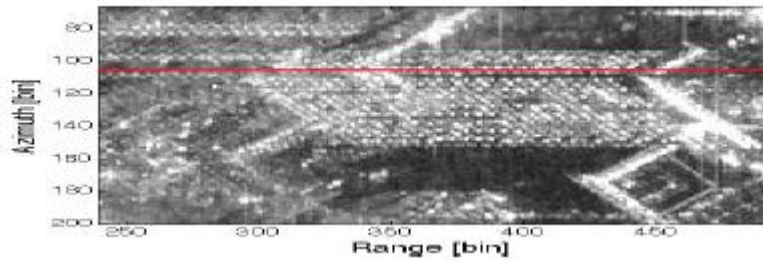
$$\mathbf{g} = \mathbf{R}\boldsymbol{\gamma}$$

Méthodes d'inversion:

- Méthodes d'analyse spectrale
- Méthodes parcimonieuses



SAR tomography



Porfiri et al., Multitemp 2015

Overview

■ How recovering elevation information ?

- Radargrammetry
- Interferometry
- Tomography

■ Focus on urban areas

- Geometric limits
- Use of external information

■ How helping with image processing ?

- Data and prior models
- Fusion of information

■ Conclusion



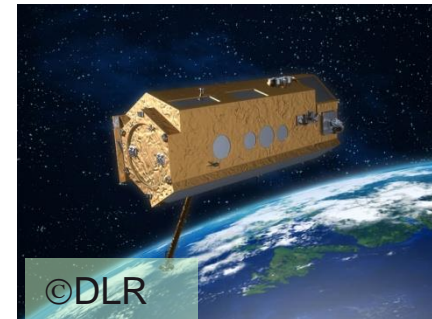
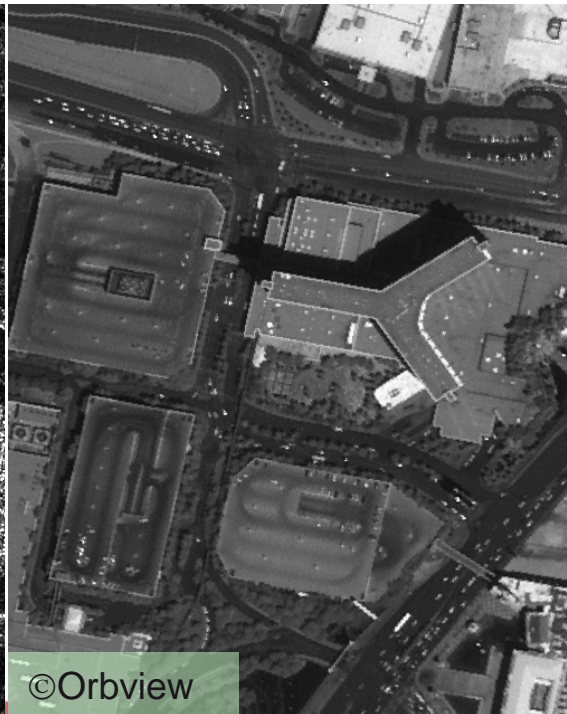
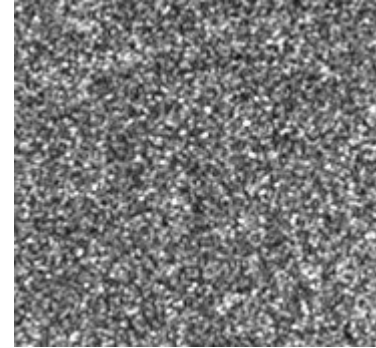
TerraSAR-X
DLR project
LAN 176



Urban areas

■ SAR images :

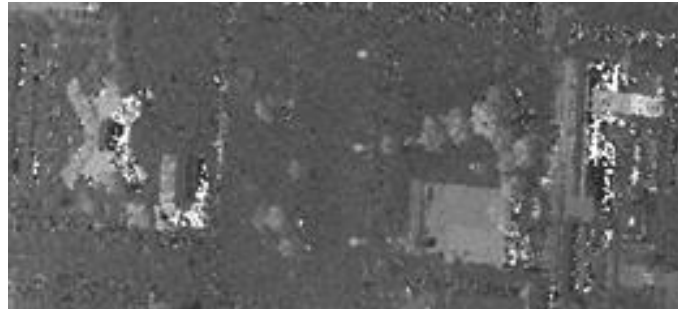
- Speckle noise
- Strong influence of geometry (incidence angle / object geometry)



Challenges of urban areas

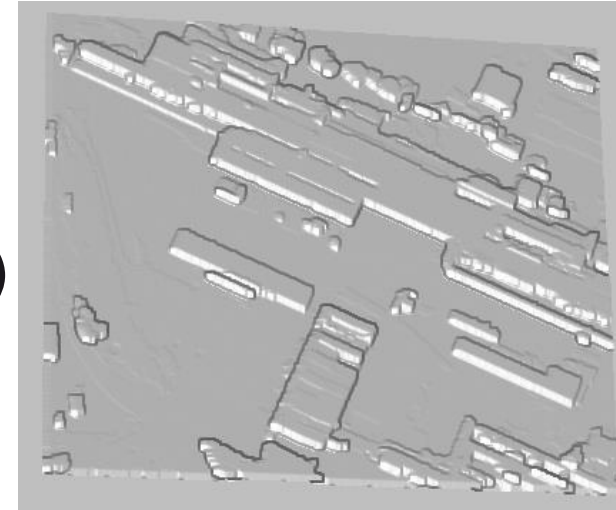
■ Geometric difficulties

- Shadow areas
- Overlay areas



■ Solutions

- Multi-aspect images (asc/desc)
- SAR tomography
- Combination with other data (SAR, optic)
- Image processing methods



Overview

■ How recovering elevation information ?

- Radargrammetry
- Interferometry
- Tomography

■ Focus on urban areas

- Geometric limits
- Use of external information

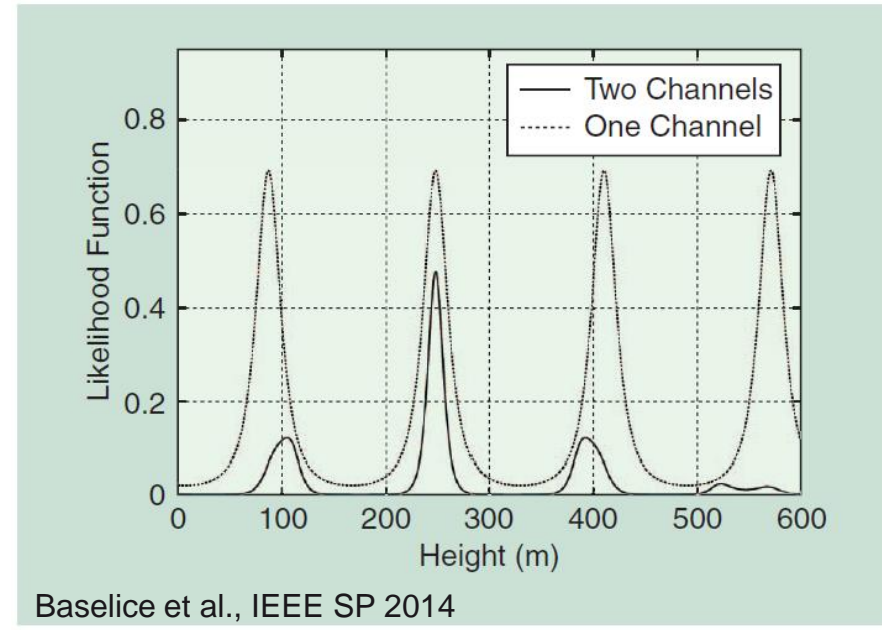
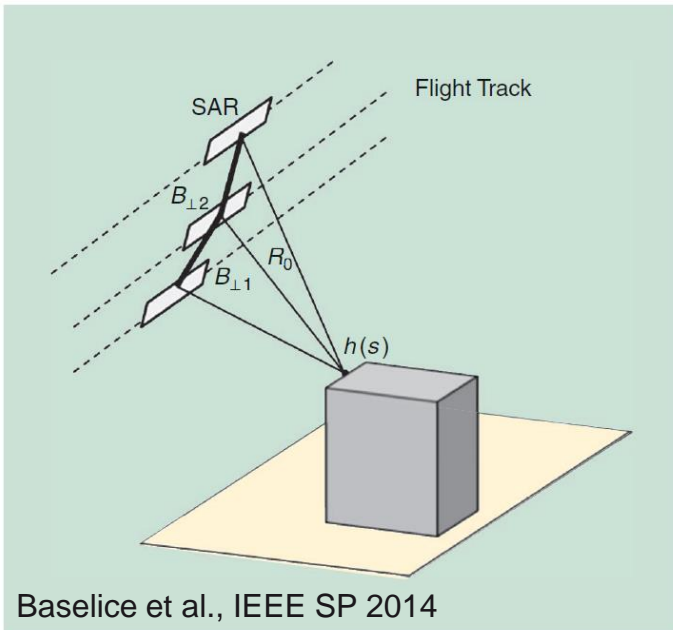
■ How helping with image processing ?

- Data and prior models
- Fusion of information

■ Conclusion



Multi-channel InSAR data



$$\Sigma = R \begin{pmatrix} 1 & \gamma_{1,2} \exp(j\psi_{1,2}) & \cdots & \gamma_{1,D} \exp(j\psi_{1,D}) \\ \gamma_{1,2} \exp(-j\psi_{1,2}) & 1 & & \gamma_{2,D} \exp(j\psi_{2,D}) \\ \vdots & & \ddots & \vdots \\ \gamma_{1,D} \exp(-j\psi_{1,D}) & \gamma_{2,D} \exp(-j\psi_{2,D}) & & 1 \end{pmatrix}.$$

Image processing methods

■ Formulation of a global optimization problem:

$$\hat{h}^{(R-NL)} = \arg \min_h - \sum_i \lambda_i \log \det(\Sigma_i(h_i)) + \lambda_i \text{tr}(\Sigma_i(h_i)^{-1} C_i) + \sum_{(i,j)} |h_i - h_j|$$

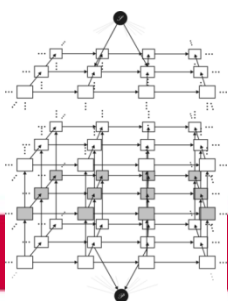
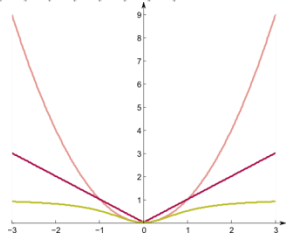
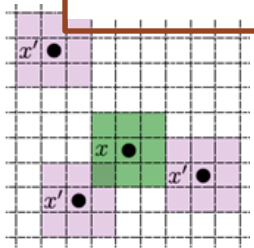
■ Likelihood term: exploiting image redundancy

- NL-SAR based regularization

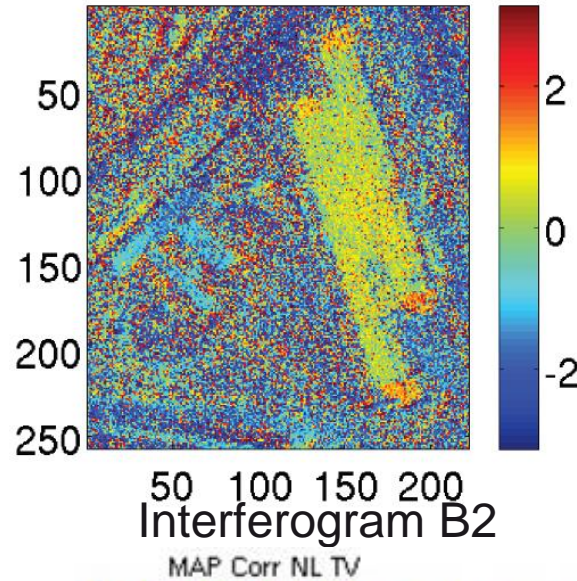
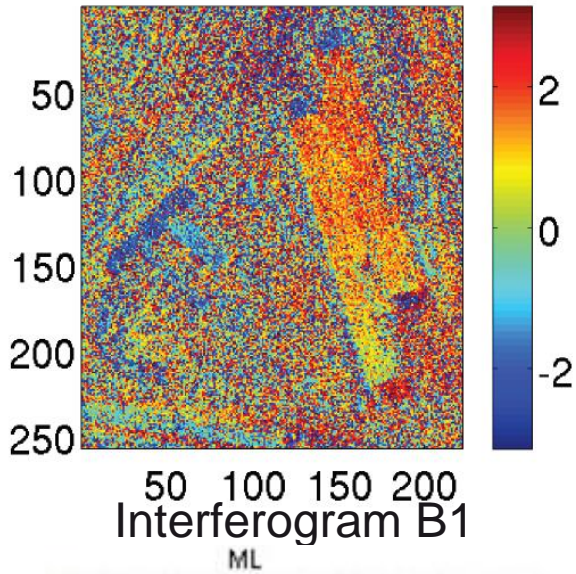
■ Prior term: exploiting elevation regularity

- Enforce smooth reconstruction with discontinuities

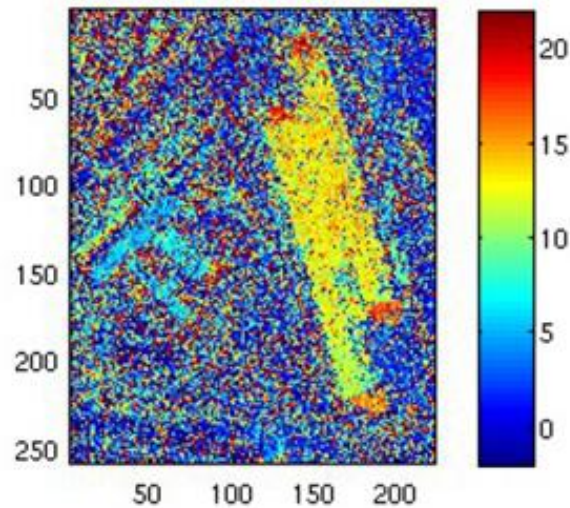
■ h optimization: graph-cut based algorithm



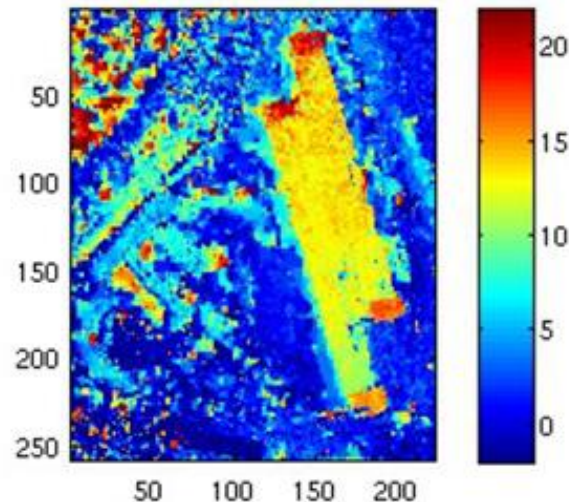
Multi-baseline InSAR



Non-local + total
variation regularization
(3 CSK data)
[Deledalle et al. 2015]



Without regularization



With regularization



Conclusion

■ Well-established approaches:

- Differential interferometry and « permanent scatterer » -like methods
- Multi-aspect fusion

■ Still challenging

- Dealing with few interferograms
- Obtaining a dense reconstruction
- Combining with other data



Références (1)

- G. Ferraioli, C. Deledalle, L. Denis, F. Tupin, *Patch based estimation and regularized inversion for multi-baseline interferometry*, IEEE TGRS (submitted, 2017)
- Ch.-A. Deledalle, L. Denis, F. Tupin, A. Reigber and M. Jäger, *NL-SAR: a unified Non-Local framework for resolution-preserving (Pol)(In)SAR denoising*, IEEE Transactions on Geoscience and Remote Sensing, 2015
- F. Ponton, E. Trouvé, M. Gay, A. Walpersdorf, R. Fallourd, J. M. Nicolas, F. Vernier and J.-L. Mugnier, *Observation of the Argentière Glacier Flow Variability from 2009 to 2011 by TerraSAR-X and GPS Displacement Measurements*, IEEE Journal of Selected Topics in Applied Earth Observations and Remote Sensing, 2014
- H. Sportouche, F. Tupin and L. Denise, *Extraction and 3D Reconstruction of Isolated Buildings in Urban Scenes from High-Resolution Optical and SAR Spaceborne Images*, IEEE Transactions on Geoscience and Remote Sensing, 2011
- L. Denis, F. Tupin, J. Darbon and M. Sigelle, *Joint Regularization of Phase and Amplitude of InSAR Data: Application to 3D reconstruction*, IEEE Transactions on Geoscience and Remote Sensing, November 2009
- F. Tupin and M. Roux, *Markov Random Field on Region Adjacency Graphs for the fusion of SAR and optical data in radargrammetric applications*, IEEE Transactions on Geoscience and Remote Sensing, 2005

Références (2)

- Radargrammetric DEM Extraction Over Urban Area Using Circular SAR Imagery, Stephan Palm, Hélène M. Oriot, and Hubert M. Cantalloube, IEEE TGRS 2012
- Radargrammetric Processing for 3-D Building Extraction from High-Resolution Airborne SAR Data, E. Simonetto, H. Oriot, H. cantalloube, IEEE TGRS 2005
- [Fornaro et al. 2009] G. Fornaro, D. Reale, F. Serafino, Four-Dimensional SAR Imaging for Height Estimation and Monitoring of Single and Double Scatterers, IEEE TGRS, 2009
- [Fornaro et al. 2014] Tomographic processing of interferometric SAR data, IEEE Signal Processing Magazine, 2014
- [Yan et al. 2012] Mexico city subsidence measured by InSAR time series: joint analysis using PS and SBAS approaches, IEEE JSTARS 2012
- [Zhu Bamler 2014], Superresolving SAR tomography for multidimensional imaging of urban areas: compressive sensing-based Tomo-SAR inversion, IEEE Signal Processing Magazine, 2014
- [Zhu Bamler 2009] Very High Resolution SAR tomography via compressive sensing, Fringe'09
- [Porfiri et al., 2015] Building profile reconstruction using TSX time series and tomographic techniques, Multitemp 15